16th World Conference on Earthquake Engineering, 16WCEE 2017

Santiago Chile, January 9th to 13th 2017

Paper N° 4256

Registration Code: S-Z1462974398

An evaluation of stress-softening behaviour of HDNR bearings on the seismic response of base-isolated structures

E. Tubaldi[1], H. Ahmadi[2], A. Muhr[2], L. Ragni[3], A. Dall'Asta[1]

(1) *Marie Curie Research Fellow, Department of Civil and Environmental Engineering, Imperial College London, London, UK; email: etubaldi@ic.ac.uk*

(2) *Tun Abdul Razak Research Centre (TARRC), Brickendonbury, Brickendon Lane, Hertford SG13 8NL, UK hahmadi@tarrc.co.uk; amuhr@tarrc.co.uk*

(3) *Department of Civil and Building Engineering and Architecture, Polytechnic University of Marche, Via Brecce Bianche Ancona (AN), Italy; E-mail: laura.ragni@univpm.i.*

(1) *Full professor,School of Architecture and Design, University of Camerino, Viale della Rimembranza, 63100 Ascoli Piceno (AP), Italy; E-mail: andrea.dallasta@unicam.it*

Abstract

In the last few decades, high damping natural rubber (HDNR) bearings have been extensively employed for seismic isolation of bridges and buildings because of their low horizontal stiffness and high damping capacity, which allows shifting the vibration period of the isolated structure away from where the earthquake input has the highest energy content and at the same time controlling the motion of the system. In HDNR material, filler is added to the natural rubber in order to improve its properties such as stiffness and dissipative capacity. The addition of the filler induces also a stress-softening behavior, known as "Mullins effect". This effect makes the response of HDNR bearings path-history dependent and thus may influence the seismic performance of isolated systems. Published literature has suggested that the initial "virgin" properties of the material are eventually recovered. Accordingly, current seismic codes make the assumption that "Mullins effect" is a reversible phenomenon. The present work aims at studying the consequences of such strain-history dependent behavior on the seismic response of structural systems isolated with HDNR bearings. In particular, the first part of the paper reports a wide experimental campaign carried out on a large number of virgin rubber samples in order to better investigate some aspects of the stress-softening behavior of filled rubber, such as the direction-dependence and the recovery prosperities, and to characterize the stable and transient response under different strain histories. Test results are used to define a model for simulating the behavior of HDNR bearings in shear, which is an advancement in the description of both the stable and the transient behaviors. The proposed model has been used to analyze the seismic response of a simplified isolated structure modeled as a S-DOF (single degree of freedom) system under ground motions with different characteristics and by considering two different conditions for the bearings: one assuming the virgin (or fully recovered) rubber properties and the other assuming the stable (or fully scragged) rubber properties. The obtained results show that, except for the special case of near-fault (NF) ground motions, the differences between the responses are limited although not negligible, whereas for NF records, the assumption of the virgin (or fully recovered) condition significantly reduces the effect of this type of motion on isolated structures.

Keywords: Mullins effect, stress-softening, high damping rubber, seismic isolation

1. Introduction

The seismic response of a system isolated with high-damping natural rubber (HDNR) bearings is mainly controlled by the HDNR material behavior in shear, which is characterized by different specific features such as the dependency on the strain-amplitude (Payne effect) and strain-rate, stiffening at large strains due to crystallization, stress-softening due to repeated cycles, as well the dependency on environmental factors such as ageing and ambient temperature. In particular the stress-softening, on which this paper is focused, may be considered as a macroscopic consequence of an internal process which evolves in the virgin rubber during the deformation path and is named in the literature as the "Mullins effect" [1] or "effect of scragging". It has been often considered in the past that stress-softening effects can be eliminated by subjecting the devices to several cycles at a large shear amplitude, as part of a manufacturer's quality control practices. However, experimental evidence has shown that the rubber can recover its initial (i.e. virgin) stress-strain properties over time [2-4]. The recovery behavior is usually rapid at the beginning, and then continues at slower rates. It is known that the rate of the recovery depends on different features, such as the elastomeric compound, the manufacturing process and the temperature, even if comprehensive studies on this topic have not been carried out yet. Nevertheless, since an earthquake may occur after a long period of rest of the isolation system, the virgin properties of bearings can be considered recovered, thus the evaluation of the seismic reliability of isolated structures would require dynamic analyses accounting for the occurrence of stress-softening during the strong motion.

In the last decades, several phenomenological models have been proposed to describe the behavior of HDNR bearings in simple shear [5-9] also considering the bidirectional horizontal response [10]. The presence of the axial load on the bearing has little effect on the shear load-deflecton behaviour unless it approaches the uplift/cavitation limit at the low end, or the buckling instability criterion at the high end, when more complex and variable stress states of the isolation device will arise. Thus, phenomenological models for shear force-deflection behaviour can be still used to reliably describe the global shear seismic response of isolation bearings under constant axial loads [11]. Advanced models have also been recently developed [12,13] to simulate the three-dimensional behavior of bearings, by also accounting for specific phenomena such as the cavitation occurring under tensile strains [14]. Very few models among those mentioned take into account the stress-softening process occurring during cyclic loadings. In particular, in the model proposed by [6] and then adopted in [12] this process is accounted for in a simplified way by introducing an additional elastic force which disappears when the current shear strain is within the minimum and maximum strains already experienced in the past. Differently, in [7,9,10] the stress-softening is properly modeled by using load-history dependent parameters [7] or damage parameters evolving as the strain history progresses [9,10]. However, recent experimental investigations have shown that the stress-softening is direction-dependent, in the sense that cyclic loadings in one-side direction marginally affect cyclic loadings in the other side direction [15,16]. This direction-dependent behavior, which may influence significantly the response of HDNR bearings under generic strain histories, is a subject of very recent researches and has not yet been included in device models.

In this paper, some results of an experimental campaign carried out in order to better understand and model the stress-softening affecting the seismic response of virgin HDNR isolation bearings and involving a large number of virgin material specimens are illustrated. In particular, a commonly used highly dissipative compound manufactured by TARRC (Tun Abdul Razak Research Centre), that satisfies the prescriptions of the current European code for anti-seismic devices [17] about the stability of shear properties under repeated cycling, is adopted for the specimens. Experimental results are used to define a one-dimensional non linear process-dependent constitutive model, which is an advancement of the model previously developed by some of the authors for HDNR devices [9]. In particular, the proposed model provides a better description of the transient behavior of the virgin rubber taking into account also the direction-dependence of the Mullins effect, as experimentally observed. In the last part of the paper the proposed model is employed to evaluate the influence of the stress softening on the seismic response of isolated structures. In particular, numerical investigations are carried out by considering an isolated structure modeled as a S-DOF (single degree of freedom) system and by performing several dynamic analyses under different seismic inputs, including near-fault (NF) and far-field (FF) records, producing different strain paths. In all the analyses, in order to highlight the influence of the Mullins effect, two different limit conditions have been considered: (i) the case of virgin bearings and (ii) the case where

the stress-softening is already fully developed. Although this last case may not be a realistic condition for the rubber, given the long interval time between earthquakes, it is considered as a limit case to highlight the effects of the stress-softening on the seismic response of isolated structures and to evaluate the differences between the responses obtained considering or neglecting the Mullins effect. In any case the scragged condition could be the most realistic for modeling the response during construction or soon after completion for those bearings which are subjected to large shear strains in production tests.

2. HDNR constitutive model and simulation of experimental tests

The proposed model provides a relation between the shear strain γ and the shear stress τ, based on which the force-displacement relationship of the bearing can be evaluated through simple geometrical considerations. In particular, the stress-strain material response is decomposed into two contributions:

$$\tau = \tau_0 + \tau_m \tag{1}$$

where the former (τ_0) is the stable component not affected by the strain history, whereas the latter (τ_m) describes the transient contribution which declines as the stress-softening increases during the strain history. The component τ_0 of the stress is generally described by assuming a rheological model consisting of a nonlinear elastic spring, able to describe the non linear hardening behaviour of the rubber at large strains, acting in parallel with different elements, describing the dissipative component of the response. In particular, this model employs two rate-dependent elements in parallel with the elastic spring to describe the dissipative response of the rubber and can be expressed in the form:

$$\tau_0 = \tau_e(\gamma) + \tau_{v1}(\gamma, \dot{\gamma}, \dot{\gamma}_{v1}) + \tau_{v2}(\gamma, \dot{\gamma}, \dot{\gamma}_{v2}) \tag{2}$$

where τ_e represents a nonlinear elastic contribution, τ_{v1} is the main dissipative contribution while τ_{v2} is a viscous contribution sensitive to the strain rate. The elastic contribution is given by

$$\tau_e(\gamma) = a\gamma^5 + b\gamma^3 + c\gamma \tag{3}$$

For the main dissipative contribution τ_{v1}, a modified bounding surface model (BSM) with vanishing elastic region firstly developed by [18] and used also by other authors [10,19] is adopted in series with a dashpot, in order to include the relaxation property of the material. As a consequence of this assumption, and the elastic region being vanishing, the plastic shear strain γ_p is the difference between the total shear strain γ and the inelastic strain γ_{v1}, whose rate is controlled by the following evolution law

$$\dot{\gamma}_{v1} = \nu_1 \tau_{v1} \tag{4}$$

where ν_1 is the parameter controlling the long relaxation time. The stress is provided by an incremental law, where the shear stress rate $\dot{\tau}_{v1}$ is obtained from the plastic shear strain rate $\dot{\gamma}_p = (\dot{\gamma} - \dot{\gamma}_{v1})$ through the relation

$$\dot{\tau}_{v1} = E_p \dot{\gamma}_p \tag{5}$$

The parameter E_p is the varying plastic modulus describing the non linear behaviour of the rubber from the yielding surface (vanishing in this case) to the bounding surface (R) which may be written as:

$$R = \xi_0 + \xi_1 \gamma_p^2 \tag{6}$$

The expression for the plastic modulus may have many different forms; in this paper one similar to [10] is used:

$$E_p = E_{p0}(\gamma) + \xi_2 \delta = \frac{dR}{d\gamma_p} sign\dot{\gamma}_p + \xi_2 \delta = 2\xi_1 \gamma_p sign\dot{\gamma}_p + \xi_2 \delta \tag{7}$$

where E_{p0} (γ) is the value of the plastic modulus on the bounding surface, while δ is the distance between the current stress and the bounding surface, which is positive in loading processes (when $\dot{\gamma}$ >0) and negative in unloading processes (when $\dot{\gamma}$ <0), as expressed by the following equation:

$$\delta = \left| Rsign\dot{\gamma}_p - \tau_{v1} \right| \tag{8}$$

However, differently from [10] and in order to better fit the experimental results, it has been assumed that the parameter ξ_2 controlling the dependence of the plastic modulus on the distance δ depends linearly on the modulus of the current plastic deformation, according to the following expression:

$$\xi_2 = \xi_{2,1} + \xi_{2,2} \left| \gamma_p \right| \tag{9}$$

Finally, the term τ_{v2} is a viscous contribution sensitive to the strain rate, given by

$$\tau_{v2}(\gamma, \gamma_{v2}) = E_{v2}(\gamma - \gamma_{v2}) \tag{10}$$

where γ_{v2} describes the inelastic strain and its evolution law, depending on the parameter ν_2 which controls the short relaxation time, is:

$$\dot{\gamma}_{v2} = \nu_2 \tau_{v2}(\gamma, \gamma_{v2}) \tag{11}$$

Stress-softening models are usually based on "damage" parameters that reduce the material response [7,9,10]. The model proposed in this paper, is based on a damage parameter q_e affecting the elastic response (τ_e) and which progressively grows, pointing to a limit value which varies with the current total strain. In this way the different stable loops are obtained when strain cycles involve different maximum strains, as experimentally observed. However, in order to account for the direction dependence of the stress-softening, as highlighted by the experimental results, two separate damage parameters q_e^+ and q_e^- evolving only for positive and negative strains respectively are introduced. A minor damage effect concerns the reduction of the cycle amplitude at zero strain, as measured by the stress intercept. This latter effect cannot be related to an elastic contribution, which is null for zero strains, thus the response reduction is due to a further damage mechanism, described by the parameter q_v involving the dissipative response (τ_{v1} and τ_{v2}). It is worth noting that the direction dependence of the damage pertains to the elastic contribution only and cannot be assumed for q_v, because this would lead to discontinuities in the shear stress by passing from positive to negative strain amplitudes which are not observed in the experimental tests. Thus, this parameter evolves both for positive and negative strains so that the response in the negative direction is slightly affected by cycling at the positive direction, as observed in the experimental tests. If it is assumed that the initial response is proportional to the stable contribution, the two damaged contributions affecting the elastic response along the two directions and the damage contribution affecting the dissipative response can be expressed by the following relations

$$\tau_{me} = \alpha_e (1 - q_e^+) \tau_e \text{ for } \gamma > 0 \tag{12a}$$

$$\tau_{me} = \alpha_e (1 - q_e^-) \tau_e \text{ for } \gamma < 0 \tag{12b}$$

$$\tau_{mv} = \alpha_v (1 - q_v)(\tau_{v1} + \tau_{v2}) \tag{12c}$$

It is assumed that the evolution of all damage parameters is proportional to the strain rate, i.e. they evolve as the strain history progresses, and that their limit value depends on the current value of strain. In particular, the

evolution laws of the elastic damage parameters for $\gamma > 0$ may be posed in the following form:

$$\dot{q}_e^+ = \zeta_e |\dot{\gamma}| \left(\left(\frac{|\gamma|}{\gamma_{\text{mod}}} \right)^\beta - q_e^+ \right) \qquad \text{if} \quad q_e^+ < \left(\frac{|\gamma|}{\gamma_{\text{mod}}} \right)^\beta \tag{13a}$$

$$\dot{q}_e^+ = 0 \qquad \text{if} \quad q_e^+ \geq \left(\frac{|\gamma|}{\gamma_{\text{mod}}} \right)^\beta \tag{13b}$$

$$\dot{q}_e^- = 0 \tag{13c}$$

whereas for $\gamma < 0$ the evolution law of $\dot{q}_e^+$ and $\dot{q}_e^-$ are inverted. During a cyclic strain history both the damage parameters q_e^+ and q_e^- tend to the same limit value, depending on the amplitude of the strain cycle and the velocity of the damage evolution is controlled by the parameter ζ_e. In particular, the maximum value that can be reached by q_e^+ and q_e^- for cycles not exceeding $|\gamma|$ is given by the expression $\left(|\gamma|/\gamma_{\text{mod}}\right)^\beta$ where γ_{mod} is the maximum amplitude for which the model is deemed valid (2.5 for this model). It should be noted that the damage parameters can only increase and Eqn13b prevents further increase once their limit has been attained. Finally, for the damage parameter q_v a similar evolution law is assumed but with a different velocity parameter (ζ_v) and without the dependence on the strain direction:

$$\dot{q}_v = \zeta_v |\dot{\gamma}| \left(\left(\frac{|\gamma|}{2.5} \right)^\beta - q_e^+ \right) \qquad \text{if} \quad q_v < \left(\frac{|\gamma|}{\gamma_{\text{mod}}} \right)^\beta \tag{14a}$$

$$\dot{q}_v = 0 \qquad \text{if} \quad q_v \geq \left(\frac{|\gamma|}{\gamma_{\text{mod}}} \right)^\beta \tag{14b}$$

Material parameters adopted for the model, calibrated on the basis of the experimental tests reported in the following, are given in Table 1 and Table 2 for the stable and transient response respectively.

Table 1 – Model parameters of the stable response

τ_e			τ_{v1}					τ_{v2}	
E	b	C	ξ_0	ξ_1	$\xi_{2,1}$	$\xi_{2,2}$	ν_1	E_2	ν_2
N/mm^2	N/mm^2	N/mm^2	N/mm^2	N/mm^2	-	-	mm^2/Ns	N/mm^2	mm^2/Ns
0.015	-0.05	0.28	0.14	0.08	3.5	1.5	0.4	0.068	8.5

Table 2 - Model parameters of the transient response

τ_{me}			τ_{mv}		
α_e	ζ_e	β	α_v	ζ_v	β
-	-	-	-	-	-
1.7	0.25	0.4	2.2	0.125	0.4

In Figure 1a the simulation of a symmetric cyclic test with constant strain rate (equal to 1s^{-1}) carried out at the maximum strain amplitude 2.5 and followed by cycles with smaller amplitudes (equal to 2, 1.5, 1, 0.5 and 0.25) is reported. The agreement between experimental and numerical results is very satisfactory both for

the first cycles at the maximum strain amplitude and for the stable cycles at different strain amplitudes, confirming the ability of the model to simulate both the transient and stable response. In Figure 1b the simulation of an asymmetric test consisting of cycles with constant strain rate (equal to $2s^{-1}$) and positive strains (at strain amplitude 1.5) followed by cycles with negative strain (at strain amplitude 1.5) is reported. In this case, the agreement between the experimental and numerical results confirms the ability of the proposed model of simulating the direction-dependence of the Mullins effect. Figure 2 reports the simulation of cyclic tests with constant strain rate (equal to $4s^{-1}$) characterized by different values of the maximum deformation imposed, equal to 2 (Figure 2a), 1.5 (Figure 2b), 1 (Figure 2c) and 0.5 (Figure 2c). This comparison confirms the ability of the model to simulate stable cycles which have different stiffness after different maximum deformations have been experienced. Finally, the ability of the model to describe the seismic response of isolated structures has been checked by simulating two further tests, where strain histories reported in Figure 3 are imposed, representing the simulated displacement responses of a S-DOF isolated structure under a near-fault (Figure 3a) and a far-field (Figure 3b) record prior and after a scragging procedure (included in the strain histories) carried out at the maximum shear strain of 2.5. In all the cases the simulated stress response is very close to the experimental stress behavior observed when the same strain-history is applied to a double shear testpiece, as can be observed in Figure 4.

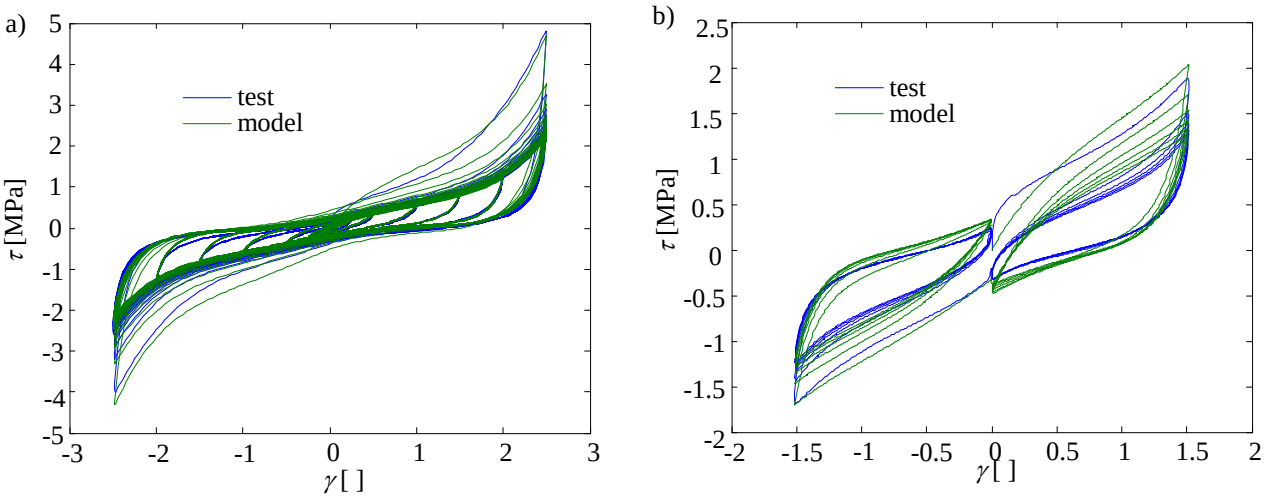

Figure 1 – Simulation of a symmetric (a) and asymmetric (b) test

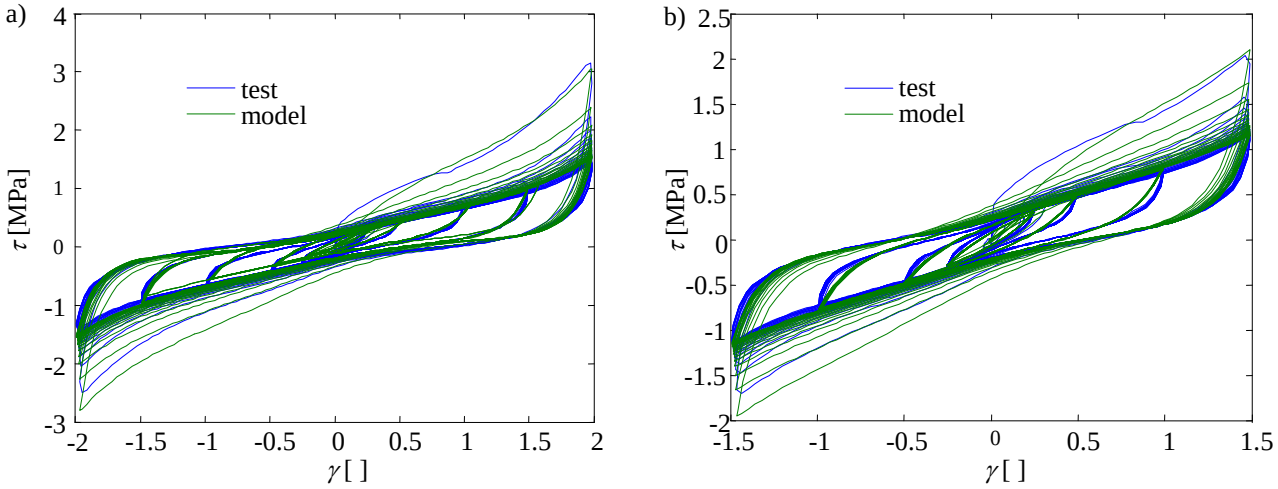

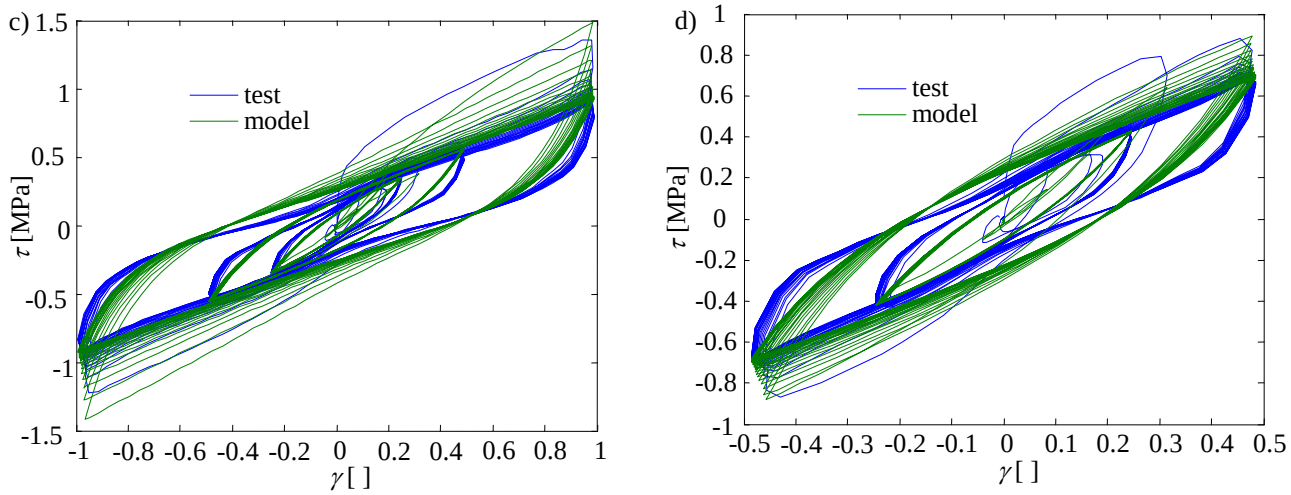

Figure 2– Simulation of tests with different maximum strain amplitudes

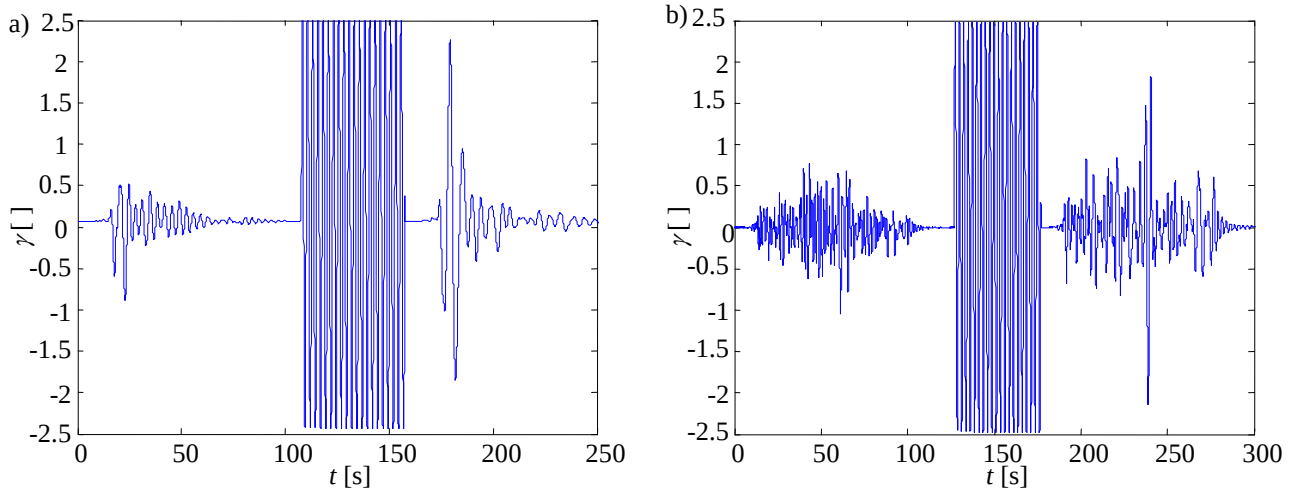

Figure 3 – Imposed strain histories before and after a scragging procedure simulating the response under (a) a near fault and (b)a far-field record.

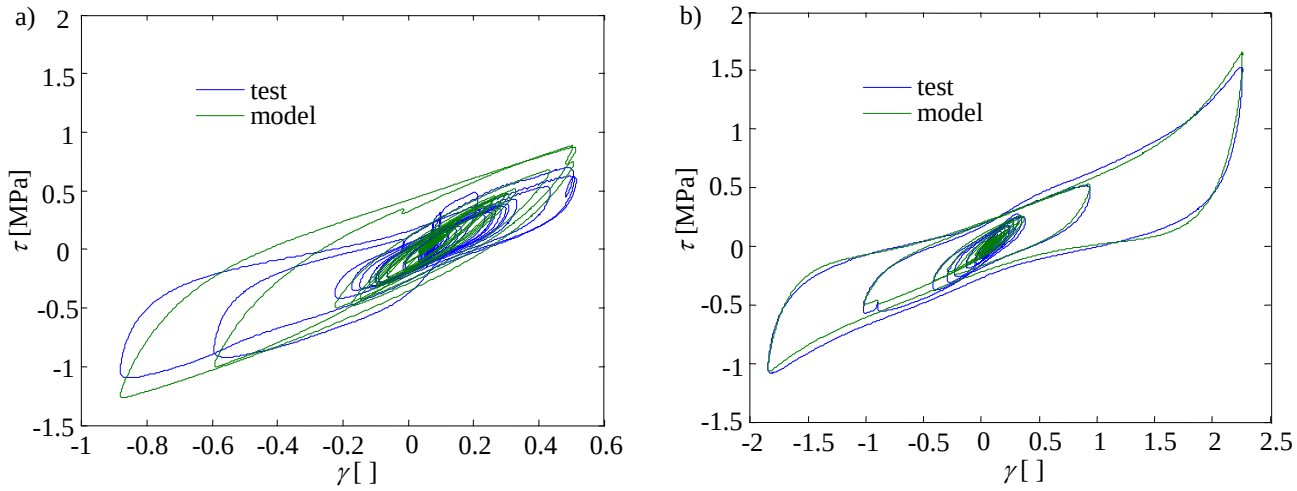

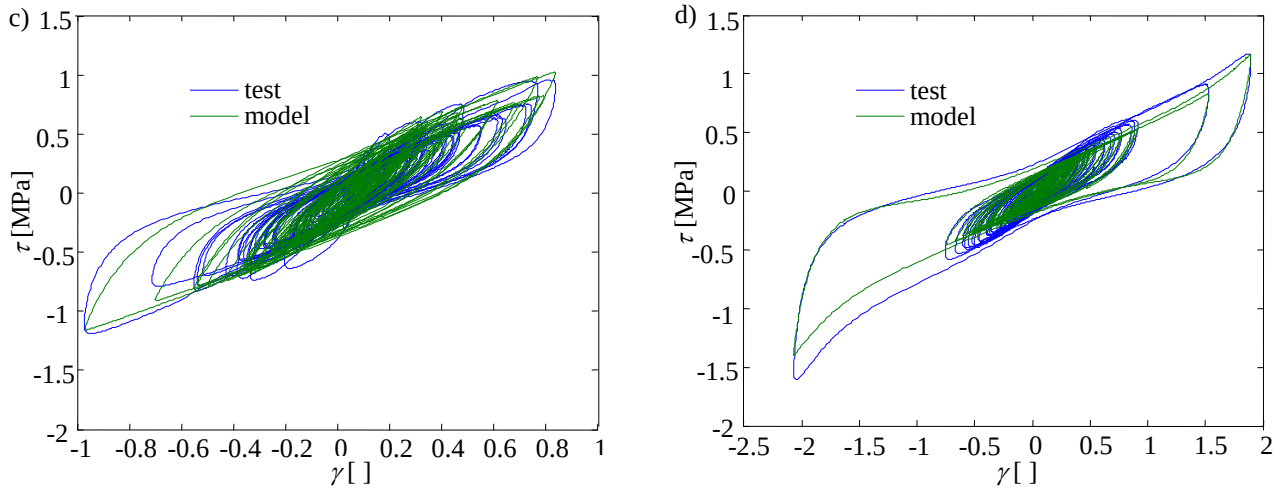

Figure 4 – Simulation of seismic tests under a near fault (a,b) and a far-field (c,d) record.

3. Seismic response of structures isolated by HDNR bearings

The case study considered in this paper consists of an isolated structure modelled as a S-DOF system, with a total mass equal to M=800 kNs^2/m. For the isolation system a rubber thickness equal to h=0.138 m is chosen to have a maximum shear strain of approximately 1.5 under a realistic value of the maximum displacement equal to 0.2m. The isolation system is finally defined by the total rubber area assumed equal to A=0.917 m^2, which permits to obtain a vibration period of about T_{is}=2 s (considering an effective shear modulus G_{eff}=1.19 N/mm^2, which is the average value between the effective shear modulus related to the first and the third cycle at the design shear amplitude and frequency). In order to evaluate the effects due to the load-history dependence, several ground motions are considered. In particular, two sets of ground motion records are analyzed separately, one representative of far field (FF) and the other of near-fault (NF) seismic inputs. In order to compare results coming from different seismic inputs, the selected ground motions have been scaled iteratively to achieve a maximum value of the displacement equal to 0.2m, corresponding to the design strain amplitude γ_{is} =1.5.

Table 3. Far-field ground motions.

Name	Event	Station	M	R_{rup}(km)	Component	PGA (g)	SF
FF1	Northridge-01	Beverly Hills - 12520 Mulhol	6.69	18.36	H1	0.535	1.87
FF2	Northridge-01	Beverly Hills - 14145 Mulhol	6.69	17.15	H1	0.440	0.80
FF3	Northridge-01	Castaic - Old Ridge Route	6.69	20.72	H1	0.505	1.19
FF4	Imperial Valley-06	Delta	6.53	22.03	H1	0.262	1.47
FF5	Imperial Valley-06	Delta	6.53	22.03	H2	0.262	1.26
FF6	Imperial Valley-06	El Centro Array #13	6.53	21.98	H1	0.118	3.65
FF7	Imperial Valley-06	Niland Fire Station	6.53	36.92	H1	0.088	5.32
R_{rup}= Closest distance to rupture plane, SF= scale factor							
H # =component name							

Table 4. Near-fault ground motions.

Name	Event	Station	M	R_{rup}(km)	Component	PGA (g)	SF
NF1	Northridge-01	Sylmar - Converter Sta	6.69	5.35	FN	0.698	0.50
NF2	Northridge-01	Sylmar - Converter Sta East	6.69	5.19	FN	0.686	0.68
NF3	Landers	Lucerne	7.28	2.19	FN	0.727	0.60
NF4	Northridge-01	Newhall - W Pico Canyon	6.69	5.48	FN	0.363	0.45
NF5	Imperial Valley-06	El Centro Array #6	6.53	1.35	FN	0.448	0.66
NF6	Imperial Valley-06	El Centro Array #6	6.53	1.35	FP	0.448	0.78
NF7	Imperial Valley-06	El Centro Array #7	6.53	0.56	FN	0.437	0.72
R_{rup}= Closest distance to rupture plane, SF= scale factor							
FN=fault normal component NP= fault parallel component							

For each analysis, in addition to the “virgin” case also the "scragged" case is considered, describing the rubber behavior when the stress-softening effect has fully exhausted at the design strain amplitude γ_{is}=1.5 (damage parameters equal to the limit value at the design strain amplitude, i.e. $\left(|\gamma|/\gamma_{mod}\right)^{\beta} = (1.5/2.5)^{0.4} = 0.82$). In Tables 5 the results of all the analyses are reported in terms of peak values of bearing shear strain γ_b and bearing shear stress τ_b obtained by considering the scragged and the virgin bearing properties, for both the FF and NF records.

Table 5. Peak response values for FF and NF ground motions.

FF records					**NF records**				
	γ_b [-]		**τ_b [MPa]**			**γ_b [-]**		**τ_b [MPa]**	
	virgin	**scragged**	**virgin**	**scragged**		**virgin**	**scragged**	**virgin**	**scragged**
FF1	1.500	1.365	1.924	0.972	NF1	1.500	2.529	1.815	2.859
FF2	1.500	1.334	1.896	0.946	NF2	1.500	2.072	2.075	1.767
FF3	1.500	1.429	2.044	0.994	NF3	1.500	2.221	2.038	2.067
FF4	1.500	2.049	1.543	1.691	NF4	1.500	2.324	2.056	2.342
FF5	1.500	1.696	1.595	1.276	NF5	1.500	2.681	2.045	3.560
FF6	1.500	2.134	1.845	1.891	NF6	1.500	2.497	1.885	2.822
FF7	1.500	1.768	1.767	1.325	NF7	1.500	2.689	1.974	3.594
average	**1.500**	**1.682**	**1.802**	**1.299**	**average**	**1.500**	**2.430**	**1.984**	**2.716**

First of all, the results related to the virgin case confirm that the response for virgin bearings is significantly influenced by the load-history dependent damage process. In fact, despite in all the analyses the maximum shear strain being equal to 1.5, the corresponding shear stresses are quite different. In particular, for the FF records the maximum shear stresses obtained are significantly different to each other (from 1.543 MPa to 2.044 MPa), because response histories may be such that the Mullins effect is very important if few short-amplitude cycles take place before the largest one, or less significant if several cycles with short or large amplitude take place before the largest one. This difference is evident by also observing the shear stress-strain diagram of the virgin response (green line) reported in Figures 5a and 5b and obtained by applying two FF records, one representative of the first case (FF2) and the other representative of the second one (FF5). In contrast, in the case of NF records, the response histories are all characterized by few short-amplitude cycles before the largest one, thus the shear stresses are all high and similar to each other (from 1.815 MPa to 2.075 MPa), as can also be observed in Figures 6a and 6b, where the shear stress-strain diagram relevant to two NF records (NF3 and NF6) are illustrated.

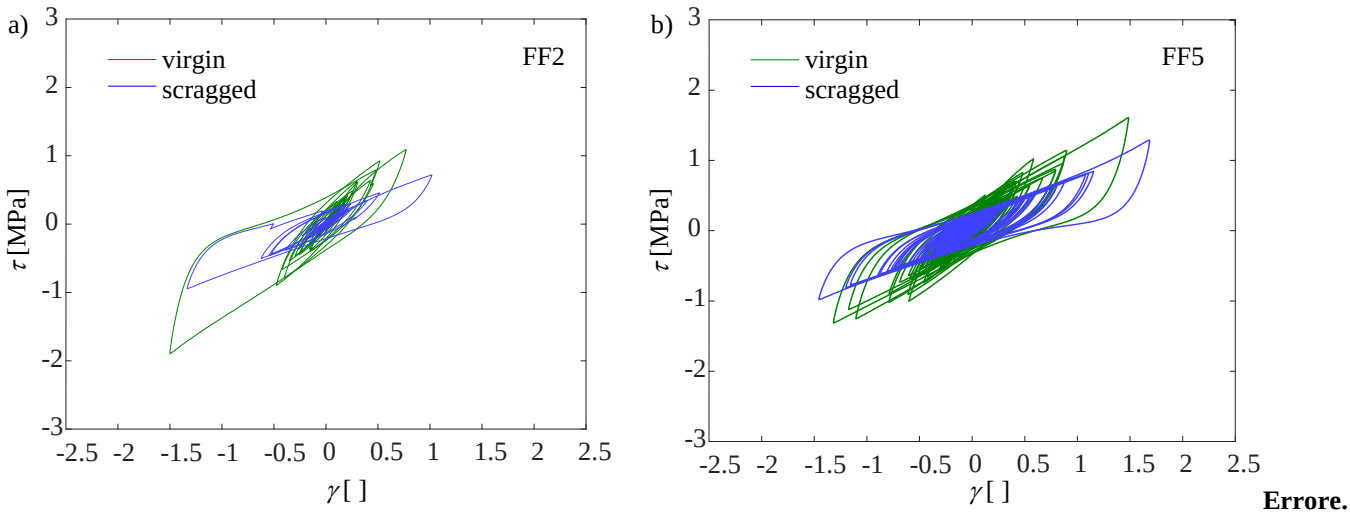

Errore. Il collegamento non è valido.

Figure 5 – Result of the analyses for two FF records

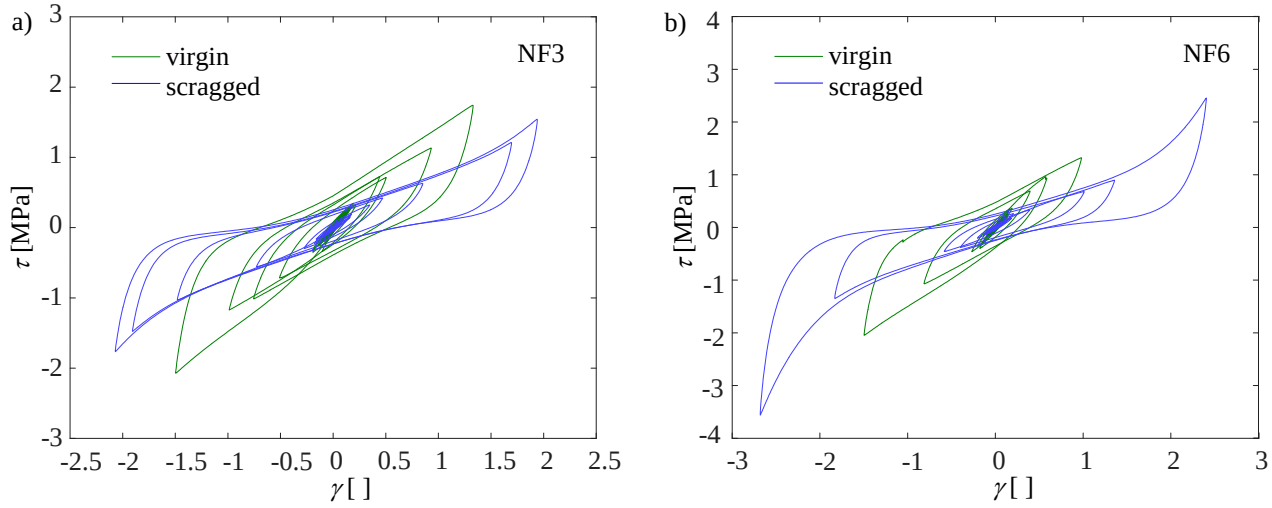

Figure 6 – Result of the analyses for two NF records

For what concerns the comparison between the virgin and scragged cases, it must be first pointed out that the FF records may exhibit constant or increasing displacement spectra at large periods, while the NF records are

always characterized by displacement spectra which increase significantly at large periods. In the case of FF records with constant spectrum, although the scragged and virgin devices have different dynamic properties, they undergo similar displacements (a little larger or smaller in the scragged case than the virgin one). Thus, being the scragged device more flexible, the maximum stresses attained in the scragged case are smaller (see FF1, FF2, FF3 in Table 5 and Fig. 5a). In contrast, for the FF records with increasing displacement spectra at large periods, the scragged bearing undergoes larger displacements than the virgin one. However, in the cases where the Mullins effect is not significant (several cycles with large amplitude taking place before the largest one) the differences are not very large and the maximum stresses attained by the scragged device remain smaller (Fig. 5b and FF5 and FF7 in Table 5). Conversely, in the case where response histories are such that the Mullins effect is maximum (only few small-amplitude cycles taking place before the largest one) the differences increase (see FF4 and FF6 in Table 5) and the maximum stresses achieved by the scragged device become larger. Under the action of NF ground motions, as a consequence of the combined effect due to the significant Mullins effect and very increasing displacement spectra, the response in terms of maximum strain of the scragged bearing is always significantly larger than the response of the virgin device, as can observed in Fig. 6a (representative of the response to NF2,NF3,NF4 records in Table 5), or even more pronounced in Fig.6b (representative of the response to NF1,NF5,NF6 and NF7 records in Table 5), where a strain amplitude in the range of the stiffness upturn of the rubber is attained by the scragged bearing. In the first case the maximum shear stresses of the virgin and scragged devices are similar, whereas in the second case the shear stress experienced by the scragged bearing becomes significantly larger. On average, in the case of FF motions the maximum strain is 12% lower for the virgin case with respect to the scragged case, whereas the maximum stress is 27% larger. Thus, as expected, neglecting evolution of stress softening during the earthquake leads to an overestimation of the displacements and an underestimation of the stresses of the bearing and thus of the forces transmitted. However, the difference between the forces is limited (lower with respect to the ratio between the first and tenth cycle at the design strain amplitude, which is about 1.6) because of the smaller displacements attained for the virgin bearings. In contrast, in the case of NF records, both the average strain and the average stress are smaller in the case where virgin rubber properties are considered. In particular, the normalized differences are respectively 62% for the strains and 37% for the stresses.

4. Conclusions

This paper reports on the experimental and numerical investigations carried out to better understand and model the stress-softening behaviour of the filled high-damping natural rubber (HDNR) and its impact on the seismic response of isolated systems. In particular, an experimental campaign, carried out at TARRC on a large number of virgin HDNR pieces, was used to fit and validate a model for simulating the behaviour of HDNR bearings in shear, which is an advancement in the description of both the stable and the transient behaviors. The proposed model has been used to analyse the seismic response of a simplified isolated structure modelled as a S-DOF system under ground motions with different characteristics for both the virgin and scragged conditions. The results showed that, except for the special case of NF ground motions, neglecting evolution of stress softening during the earthquake leads to an overestimation of displacements of the bearings and an underestimation of the stresses acting on the bearings and thus of the forces transmitted to the structure. However, these differences are limited and could justify simplified approaches, such as those based on safety factors or property modification factors to apply to simplified models (elasto-plastic or visco-elastic models) to account for the consequences of the Mullins effect. In contrast, in the case of NF records, which are usually considered very critical for isolated systems, the results show that neglecting evolution of stress softening during the earthquake results in very large displacements reaching the range of the stiffness upturn of the rubber and very high stresses acting on the bearing and superstructure. Thus the use of models accounting for the stress-softening is recommended in this case to correctly evaluate the reliability of isolated structures.

5. Acknowledgements

The study reported in this paper was sponsored by the Tun Abdul Razak Research Centre (TARRC) and by the Italian Department of Civil Protection within the Reluis-DPC Projects 2016. The authors gratefully acknowledge this financial support.

6. References

[1] Mullins L. Softening of rubber by deformation, Rubber Chemistry and Technology 1969, 42(1): 339-362.

[2] Kulak RF, Coveney VA, Jamil S. Recovery characteristics of high-damping elastomers used in seismic isolation bearings, Seismic, Shock, and Vibration Isolation, ASME Publication PVP-Vol. 379, American Society of Mechanical Engineers, Washington, D.C. 1998.

[3] Constantinou MC, Tsopelas, P, Kasalanati A, Wolff E. Property modification factors for seismic isolation bearings, MCEER Technical Report, Multidisciplinary Center for Earthquake Engineering Research, Buffalo, New York, 1999.

[4] Thomson AC, Whittaker AS, Fenves GL, Mahin SA. Property modification factors for elastomeric seismic isolation bearings. Proceedings of the 12th World Conference on Earthquake Engineering, New Zealand, Auckand, 2000.

[5] Ahmadi HR, Fuller KNG, Muhr AH. Predicting response of non-linear high damping rubber isolation systems, Proceedings of the Eleventh World Conference on Earthquake Engineering Acapulco, Mexico. 1996.

[6] Kikuchi M, Aiken ID. An Analytical Hysteresis Model for Elastomeric Seismic Isolation Bearings, Earthquake Engineering and Structural Dynamics 1997, 26(2):215-231.

[7] Hwang JS, Wu JD, Pan .C, Yang G. A Mathematical Hysteretic Model for Elastomeric Isolation Bearings. Earthquake Engineering and Structural Dynamics 2002, 31(4): 771-789.

[8] Tsai CS , Chiang TC, Chen BJ, Lin SB. An Advanced Analytical Model for High Damping Rubber Bearings, Earthquake Engineering and Structural Dynamics 2003, 32(9):1373-1387.

[9] Dall'Asta A, Ragni L. Experimental Tests and Analytical Model of High Damping Rubber Dissipating Devices, Engineering Structures 2006, 28(13):1874-1884.

[10] Grant DN, Fenves GL, Auricchio F. Modelling and analysis of High-damping Rubber Bearings for the seismic protection of bridges. Iuss Press, Pavia, 2005

[11] Yamamoto S, Kikuchi M, Ueda M, Aiken IA. A mechanical model for elastomeric seismic isolation bearings including the influence of axial load. Earthquake Engineering & Structural Dynamics 2009; 38(2): 157-180.

[12] Kikuchi M, Nakamura T, Aiken ID. Three-dimensional analysis for square seismic isolation bearings under large shear deformations and high axial loads. Earthquake Engineering and Structural Dynamics 2010, 39:1513–1531

[13] Abe M, Yoshida J, Fujino Y. Multiaxial Behaviours of Laminated Rubber Bearings and their Modeling. II: Modelling, Journal of Structural Engineering 2004;130(8):1133-1144.

[14] Kumar M. Seismic isolation of nuclear power plants using elastomeric bearings. PhD Dissertation, Departement of Civil, Structural and Environmental Engineering, University at Buffalo, 2015.

[15] Diercks N, Lion A. Modeling deformation-induced anisotropy using 1D-laws for Mullins-Effect. Constitutive models for rubber VIII, Taylor & Francis Group, London 2013, pp.419-424.

[16] Wulf H, Ihlemann J. Simulation of self-organization processes in filled rubber and their influence on anisotropic Mullins effect. Constitutive models for rubber VIII , Taylor & Francis Group, London 2013, pp.425-430

[17] European Committee for Standardization (ECS). EN 15129:2009, Anti-seismic devices, CEN, Bruxelles, 2009.

[18] Dafalias, Y., Popov, E., 1977. Cyclic loading for materials with a vanishing elastic region. Nucl. Eng. Des. 41, 293–302.

[19] Osterlof R., Wentzel H., Kari L., Diercks N., Wollscheid D. Constitutive modeling of the amplitude and frequency dependency of filled elastomers utilizing a modified Boundary Surface Model. International Journal of Solids and Structures 51 (2014) 3431–3438

[20] Jangid R. S., Kelly J. M. Base isolation for near-fault motions. Earthquake Engineering And Structural Dynamics . 2001, 30:691-707

[21] Mazza F., Vulcano A. Nonlinear Response of RC Framed Buildings with Isolation and Supplemental Damping at the Base Subjected to Near-Fault Earthquakes. Journal of Earthquake Engineering 2009, 13(5):690-715.